

Journal of Materials Chemistry B

Accepted Manuscript



This is an *Accepted Manuscript*, which has been through the Royal Society of Chemistry peer review process and has been accepted for publication.

Accepted Manuscripts are published online shortly after acceptance, before technical editing, formatting and proof reading. Using this free service, authors can make their results available to the community, in citable form, before we publish the edited article. We will replace this *Accepted Manuscript* with the edited and formatted *Advance Article* as soon as it is available.

You can find more information about *Accepted Manuscripts* in the [Information for Authors](#).

Please note that technical editing may introduce minor changes to the text and/or graphics, which may alter content. The journal's standard [Terms & Conditions](#) and the [Ethical guidelines](#) still apply. In no event shall the Royal Society of Chemistry be held responsible for any errors or omissions in this *Accepted Manuscript* or any consequences arising from the use of any information it contains.



Journal Name

ARTICLE

A Photostable AIEgen for Nucleolus and Mitochondria Imaging with Organelle-Specific Emission

Received 00th January 20xx,
Accepted 00th January 20xx

Chris Y. Y. Yu,^{ab≠} Weijie Zhang,^{ab≠} Ryan T. K. Kwok,^{ab} Chris W. T. Leung,^{ab} Jacky W. Y. Lam^{ab} and Ben Zhong Tang^{abc*}

DOI: 10.1039/x0xx00000x

www.rsc.org/

Dynamic visualization of the morphology of membrane-bounded organelles offers useful insights for studying various intracellular activities. Fluorescent probes with superior specificity and photostability are desirable for long-term tracking of these processes. In this work, we present the design and synthesis of a α -cyanostilbene derivative, abbreviated as ASCP, with aggregation-induced emission (AIE) characteristic, and its application in cell imaging. ASCP can simultaneously label mitochondria and nucleolus in live cells with distinct fluorescence, which is demonstrative of a single molecule with dual-colour organelle imaging.

1. Introduction

Nucleolus is the key structure in the nucleus. It serves as the site for ribosome synthesis and RNA assembly,¹ and is thus closely related to the cell growth and proliferation. RNA assembly occurs during the late telophase and disassembles in mitosis after the interphase.^{2–5} The details of dynamic nucleolar RNA distribution and localization throughout the cell cycle, however, have not been fully understood as dye molecules for specific labelling the RNA in live cell are rare.^{6,7} Recent reports also found that the morphology of nucleolus is associated with several neurodegenerative disorders such as Parkinson's disease.^{8,9} Thus, the development of new luminescent materials for RNA imaging in live cells is one of the hot research topics in materials science.

SYTO RNASelect is a commercial RNA-selective fluorescent probe that is commonly used for tracking the morphology change of nucleolus.¹⁰ It is virtually non-fluorescent but exhibits bright green fluorescence when bounds to RNA. However, its performance degrades easily due to its low photostability and small Stokes' shift (absorption/emission maximum: 490/530 nm). Thanks to the enthusiasm of

scientists, a variety of RNA probes have recently been developed based on oligonucleotide,¹¹ the mechanisms of fluorescence resonance energy transfer (FRET),¹² dual-labelled oligonucleotide hairpin,¹³ dual FRET molecular beacons¹⁴ and autoligation as well as fluorescent proteins.¹⁵ Unfortunately, some of them are prepared through complicated synthetic procedures and involve expensive production costs. Meanwhile, microinjection is sometimes required in cell staining, which is invasive and may cause cell damage and uneven distribution of dye molecules. On the other hand, small organic fluorophores are promising alternatives for live cell nucleolus imaging.^{16–18} For example, Chang et al. and Ge et al. designed and synthesized a series of styryl dyes and hemicyanine derivatives, respectively, for visualizing intracellular nucleolus with different emissions.^{19–21}

Mitochondria are known as the powerhouses of cell. In addition to supply cellular energy, mitochondria also play a vital role in many metabolic tasks such as regulation of membrane potential and apoptosis-programmed cell death. The morphology of mitochondria is controlled by a set of proteins. Any unexpected disruption of mitochondrial membrane is implicated of several human diseases including degenerative diseases, such as Parkinson's and Alzheimer's diseases.^{22,23} Various types of fluorescent probes that can selectively illuminate the mitochondria have been developed in order to monitor the morphology change of mitochondria and study these processes. Owing to the fact that the light emissions of these probes are often weakened by aggregate formation, they are generally used at very low concentration. However, such small numbers of dye molecules are quickly photo-bleached under continual light irradiation from the fluorescent microscope. Thus, these fluorescent probes are not capable of observing the dynamic morphology change of mitochondria in a long period of time.

^a HKUST Shenzhen Research Institute, No. 9 Yuexing 1st Road, South Area, Hi-tech Park, Nanshan, Shenzhen 518057, China. Email: tangbenz@ust.hk

^b Department of Chemistry, Hong Kong Branch of Chinese National Engineering Research Center for Tissue Restoration and Reconstruction, Institute for Advanced Study, Division of Biomedical Engineering, Division of Life Science, State Key Laboratory of Molecular Neuroscience, Institute of Molecular Functional Materials, The Hong Kong University of Science and Technology, Clear Water Bay, Kowloon, Hong Kong, China.

^c Guangdong Innovative Research Team, SCUT-HKUST Joint Research Laboratory, State Key Laboratory of Luminescent Materials and Devices, South China University of Technology, Guangzhou 510640, China.

*Electronic Supplementary Information (ESI) available: Characterization of ASCP and intermediates, and chemical structures of phospholipids used in this study. See DOI: 10.1039/c000000x/a

[†]These authors contributed equally to this work.

To achieve long-term cellular tracking, alternative systems with higher photostability are thus in urgent demand. Recently, some luminogens have been found to exhibit a phenomenon of aggregation-induced emission (AIE). These molecules are non-fluorescent in dilute solution but emit strong light in the aggregated state. The high brightness of their aggregates in aqueous solution enable them to be utilized as fluorescent visualizers for imaging organelles such as mitochondria, cell membrane, lipid droplets and lysosome.^{24–27} So far, most of the AIE probes target to an organelle specifically with a single emission colour. Therefore, two or more probes with distinct colours are needed simultaneously to co-stain different organelles. Indeed, it would be fascinating if a single AIE fluorophore can image two or more organelles with distinct emissions. Such a system can simplify the cell manipulation but until now, no such example has been reported.

In this work, we report the synthesis of a new AIE-active α -cyanostilbene derivative, namely ASCP, and its application in mitochondria and nucleolus imaging. We here demonstrate that ASCP can simultaneously label mitochondria and nucleolus in live cells with distinct fluorescence, high specificity and superior photostability.

2. Experimental Section

2.1 Materials

Tetrahydrofuran (THF; Labscan) was distilled from sodium benzophenone ketyl under nitrogen immediately before use. 1,2-Dioleoyl-sn-glycero-4-phosphocholine, 1,1',2,2'-tetraoleoyl cardiolipin (TOCL), 1,2-dioleoyl-sn-glycero-3-phospho-L-serine sodium salt, 1,2-dipalmitoleoyl-sn-glycero-3-phosphoethanolamine, and L- α -phosphatidylinositol (soy) (sodium salt), were purchased from Avanti Polar Lipids, Inc.. N-Hexanoyl-D-sphingomyelin (SM) was purchased from Sigma. Minimum essential medium (MEM), phosphate buffered saline (PBS), fetal bovine serum (FBS), sodium dodecyl sulphate (SDS), HEPES buffer, penicillin, streptomycin, MitoTracker Green and SYTO RNASelect were purchased from Invitrogen. DNA, RNA, DNase I and RNase I were purchased from Aldrich.

2.2 Instruments

¹H and ¹³C NMR spectra were measured on a Bruker AV 400 spectrometer in CDCl₃ and DMSO-*d*₆ using tetramethylsilane (TMS; δ = 0) as internal reference. Absorption spectra were measured on a Varian Cary 50 UV-Vis spectrophotometer. Steady-state fluorescence spectra were recorded on a Perkin-Elmer LS 55 spectrofluorometer with a Xenon discharge lamp excitation. Mass spectra were recorded on a GCT Premier CAB 048 mass spectrometer operated in MALDI-TOF mode. Fluorescent images were collected on a Olympus BX 41 fluorescence microscope. Laser confocal scanning microscope images were collected on Zeiss laser scanning confocal microscope (LSM7 DUO) and analyzed using ZEN 2009 software (Carl Zeiss).

2.3 Synthesis

ASCP or Compound **6** was prepared according to the synthetic route shown in scheme 1. Detailed procedures are shown below.

Synthesis of Compound 3: Into a 100 mL round bottom flask were dissolved 4-bromophenylacetonitrile (**1**; 0.69 g, 3.50 mmol) and 4-(dimethylamino)benzaldehyde (**2**; 0.81 g, 3.00 mmol) in 40 mL ethanol. Sodium hydroxide (0.14 g, 3.50 mmol) in 5 mL ethanol was then added slowly into the mixture. After stirring for 2 h, the pale yellow precipitates were filtered, washed with ethanol and dried under reduced pressure. Yield: 80%. ¹H NMR (400 MHz, CDCl₃), δ (ppm): 7.86 (d, 2H, *J* = 8.4 Hz), 7.54–7.48 (m, 4H), 7.38 (s, 1H), 6.73 (d, 2H, *J* = 8 Hz), 3.07 (s, 6H). HRMS (MALDI-TOF): *m/z* 326.0217 (M⁺, calcd. 326.0419).

Synthesis of Compound 5: Into a 100 mL two-necked round bottom flask equipped with a condenser were added **3** (0.10 g, 0.306 mmol), (4-hydroxyphenyl)boronic acid (**4**; 45 mg, 0.387 mmol), potassium carbonate (0.422 g, 3.06 mmol) and Pd(PPh₃)₄ (10 mg, 0.01 mmol) in 20 mL THF and 3 mL water under nitrogen. The mixture was stirred and heated to reflux overnight. After cooling to room temperature, the mixture was extracted with dichloromethane (DCM) for three times. The organic phase was collected, washed with water and dried over anhydrous sodium sulfate. After solvent evaporation, the crude product was purified by silica-gel column chromatography using DCM/ethyl acetate (v/v = 99:1) as eluent to furnish an orange solid as product. Yield: 74%. ¹H NMR (400 MHz, CDCl₃), δ (ppm): 8.68 (d, 2H, *J* = 4.4 Hz), 7.76–7.68 (m, 4H), 7.55 (d, 2H, *J* = 4.4 Hz), 7.26 (s, 1H), 6.74 (d, 2H, *J* = 8.4 Hz), 3.08 (s, 6H). ¹³C NMR (100 MHz, CDCl₃), δ (ppm): 150.7, 149.4, 149.3, 144.6, 142.4, 137.4, 137.5, 131.2, 130.9, 129.2, 127.0, 126.8, 125.4, 120.9, 120.9, 120.7, 111.0, 110.6, 106.0, 39.4, 39.3. HRMS (MALDI-TOF): *m/z* 325.1575 (M⁺, calcd. 325.1579).

Synthesis of Compound 6 (ASCP): Into a 100 mL two-necked round bottom flask equipped with a condenser, was dissolved **5** (50 mg, 0.154 mmol) in 5 mL acetonitrile. Iodomethane (0.1 mL) was then added and the mixture was heated to reflux for 8 h. After cooling to room temperature, the mixture was poured into diethyl ether. The dark red precipitates formed were filtered by suction filtration. The precipitates were re-dissolved in acetone and mixed with saturated KPF₆ solution (5 mL). After stirring for 1 h, acetone was evaporated by compressed air. The dark red precipitates were filtered again, washed with water and dried under reduced pressure. Yield: 95%. ¹H NMR (400 MHz, DMSO-*d*₆), δ (ppm): 8.98 (d, 2H, *J* = 6.8 Hz), 8.53 (d, 2H, *J* = 6.8 Hz), 8.18 (d, 2H, *J* = 8.4 Hz), 8.03 (s, 1H), 7.93–7.40 (m, 4H), 6.83 (d, 2H, *J* = 8.8 Hz), 4.29 (s, 3H), 3.03 (s, 6H). ¹³C NMR (100 MHz, DMSO-*d*₆), δ (ppm): 153.0, 152.0, 145.3, 144.4, 138.3, 132.0, 131.6, 128.5, 125.6, 123.5, 120.3, 118.9, 111.4, 100.3, 46.8. HRMS (MALDI-TOF): *m/z* 340.1826 (M⁺, calcd. 340.1814).

2.4 Cell Culture

HeLa cells were cultured in MEM supplemented with 10% heat-inactivated FBS, 100 units/mL penicillin and 100 $\mu\text{g/mL}$ streptomycin, in a humidity incubator with 5% CO_2 at 37 $^\circ\text{C}$. Before experiment, the HeLa cells were pre-cultured until confluence was reached.

2.5 Cytotoxicity Study

2-(4,5-Dimethyl-2-thiazolyl)-2,5-diphenyltetrazolium bromide (MTT) assay was used to evaluate the cytotoxicity of ASCP. HeLa cells (provided by American Type Culture Collection) were seeded in a 96-well plate at a density of 5000 cells per well. After 24 h incubation, the cells were exposed to a series of doses of ASCP (0–10 μM) in culture medium at 37 $^\circ\text{C}$. One day later, 10 μL of freshly prepared MTT solution was added into each well. After further incubation for 4 h, 100 μL of solubilization solution containing 10% SDS and 0.01 M HCl was added to dissolve the purple crystals. Two hours later, the absorbance at 595 nm was recorded using a Perkin-Elmer Victor plate reader. The experiment was performed at least five times.

2.6 Cell Imaging

HeLa cells were seeded on a 35 mm petri dish with a glass cover slide. After overnight cell culture, the HeLa cells were incubated in an aqueous solution of ASCP (5 μM) for 30 min or SYTO RNASelect (500 nM) for 20 min. The dye labelled-cells were washed with fresh phosphate buffered saline (PBS; pH 7.4) for three times before fluorescent imaging. For co-staining experiments, a solution of MitoTracker Green (MTG; 200 nM) was added to the HeLa cells incubated with an aqueous solution of ASCP at 15 min. After further incubation for 15 min, the dye-labelled cells were washed by fresh PBS solution for three times and then imaged by wide-field fluorescence and confocal microscopies.

2.7 Preparation of Lipid Vesicles

Chloroform stocks of different lipids (10 mg/mL) were mixed in a desired molar ratio and dried under a stream of nitrogen. The lipid films were hydrated in 25 mM HEPES buffer (pH 7.4) to a final lipid concentration of 2.2 mM. The lipid mixtures were incubated for 30 min at 37 $^\circ\text{C}$ and then sonicated for 1 h. The lipid vesicles were obtained by extruding 11 times through 100 nm pore size polycarbonate filter at 50 $^\circ\text{C}$ on a pre-warmed lipid extruder.^{28,29}

2.8. DNase and RNase Digest Tests

HeLa cells were fixed by 4% paraformaldehyde for 30 min. After incubation with 1% Triton X-100 for 2 min, the cells were permeabilized and rinsed with PBS twice. The cells were incubated either ASCP (10 μM) or SYTO RNASelect (5 μM) solution for 30 min. After washing with PBS twice, a PBS solution (100 μL) mixed with DNase (30 $\mu\text{g/mL}$) or RNase (25 $\mu\text{g/mL}$) was added and the cells were incubated in an incubator with 5% CO_2 at 37 $^\circ\text{C}$ for 2 h. The cells were rinsed by PBS twice before imaging using a wide-field fluorescence microscopy.

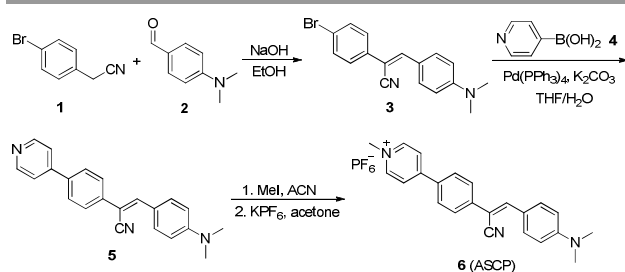
2.9 Photostability Test

Live dye-labelled HeLa cells were imaged on a confocal microscope. Conditions: excitation wavelength: 560 nm and emission filter: 650–750 nm (ASCP); excitation wavelength: 488 nm and emission filter: 500–600 nm (SYTO RNASelect).

3. Results and Discussion

3.1 Design and Synthesis of ASCP

Tetraphenylethene (TPE) and its derivatives are archetypal AIE luminogens (AIEgens). Because of their efficient emission in the aggregated state, they have been utilized as fluorescent agents for bioimaging with high sensitivity and photostability. By incorporation of a pyridinium (Py) unit to TPE, the resultant AIEgen can visualize mitochondria in HeLa cells with high specificity and bright yellow emission. To minimize the interference from autofluorescence, fluorophores with longer wavelength excitation and emission are more desirable. On the other hand, α -cyanostilbene is a good building block for generating AIEgens with different emissions by attaching various donor groups to its molecular structure. Through molecular engineering, a new AIEgen, namely ASCP, was designed. This luminogen consisted of three components: (1) α -cyanostilbene as the AIE skeleton and linker; (2) dimethylamino group as the donor to tune the emission to the red region; and (3) Py salt as the targeting agent for mitochondrion. Its synthetic procedure was described in Scheme 1. Compound **3** was synthesized by Knoevenagel condensation of 4-bromophenylacetonitrile (**1**) and 4-(dimethylamino)benzaldehyde (**2**) in basic condition. Suzuki coupling of **3** with (4-hydroxyphenyl)boronic acid (**4**) in the presence of $\text{Pd}(\text{PPh}_3)_4$ and K_2CO_3 afforded **5**. Treatment of **5** with iodomethane and KPF_6 finally furnished the desirable product ASCP in a high yield. The detailed synthesis and characterization of ASCP and the intermediates are given in Experimental Section and Fig. S1–S8 in Electronic Supplementary Information (ESI[†]).



Scheme 1. Synthetic route to ASCP.

3.2 Optical Properties

We first studied the optical properties of ASCP. Due to the hydrophilic nature of the Py salt, ASCP is soluble in polar solvents, slightly soluble in water but insoluble in nonpolar solvents such as dioxane and toluene. ASCP exhibits an

absorption band at around 450 nm, irrespective of the type of solvent used (Fig. 1A). On the contrary, it shows obvious different emission colours and intensities when the measurement was carried out in different solvents (Fig. 1B).

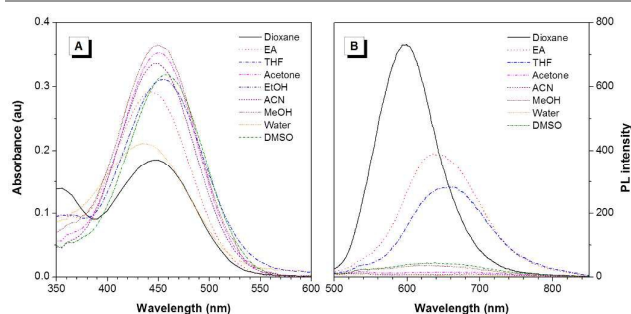


Fig. 1 (A) Absorption spectra and (B) emission spectra of ASCP in different solvents. Concentration: 10 μM ; $\lambda_{\text{ex}} = 460 \text{ nm}$.

ASCP emits a strong orange light in dilute dioxane solution. Owing to the twisted intramolecular charge transfer (TICT) effect,³⁰ the emission of the dye molecule was weakened and red-shifted with increasing the solvent polarity. In dilute DMSO solution, ASCP shows a faint red fluorescence. In contrast, gradual addition of toluene into its DMSO solution has enhanced the light emission and changed the emission colour to orange due to the gradual decrement of the solvent polarity (Fig. 2). At high toluene fraction, a much rapid fluorescence enhancement was observed due to the formation of ASCP aggregates along with the activation of the AIE process.

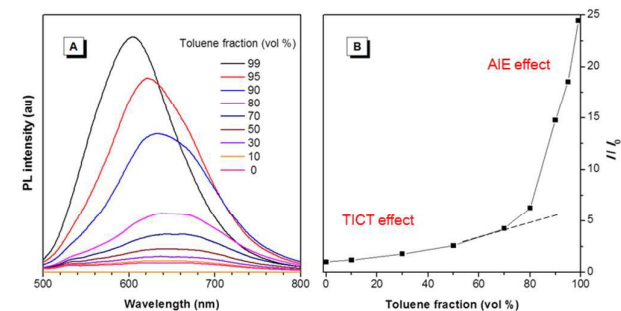


Fig. 2 (A) Emission spectra of ASCP in toluene/DMSO mixtures with different toluene fractions (f). (B) Plot of relative emission intensity (I/I_0) at 650 nm versus the composition of the toluene/DMSO mixture of ASCP. I_0 = emission intensity of ASCP in pure DMSO solution. Concentration: 10 μM ; $\lambda_{\text{ex}} = 460 \text{ nm}$.

3.3 Cell Imaging

The strong emission of ASCP in the aggregated state encourages us to utilize it as a fluorescent visualizer for mitochondrion imaging. To examine whether the dye is suitable for bio-imaging, the cytotoxicity of ASCP on HeLa cells was first evaluated using MTT assay. As depicted in Fig. 3, the cell viability remains high at ASCP concentration as high as 10 μM , suggesting that ASCP possesses a good biocompatibility. ASCP was first assessed for its capability to stain specific organelles in live HeLa cells. The HeLa cells were cultured and incubated in MEM with 5 μM ASCP for 30 min. The cells were

washed with fresh PBS and then observed under fluorescence microscope. Thanks to the high specificity of the Py unit in ASCP, the reticulum structures of mitochondria are stained with intense orange emission (Fig. 4A). To further validate the specificity of ASCP, MitoTracker Green (MTG), a commercial mitochondrial imaging agent, was used to co-stain the HeLa cells. The cell images taken on confocal microscopy illustrates that the orange fluorescence from ASCP has an excellent correlation (96.4%) with the green emission of MTG (Fig. 4D–4F).

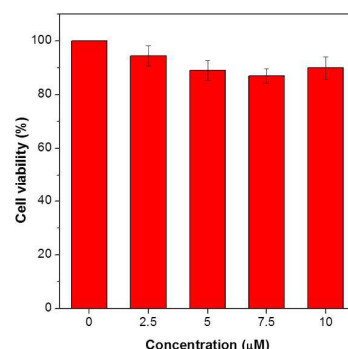


Fig. 3 Viability of HeLa cells in the presence of different concentrations of ASCP for 8 h. Data is expressed as mean value for five separate trials.

Surprisingly, by altering the focus, red fluorescence was observed in nucleolus (Fig. 4B). Thus, it seems that the two distinct fluorescence observed in from mitochondria and nucleolus is correlated with the specific interactions of ASCP with different biomolecules.

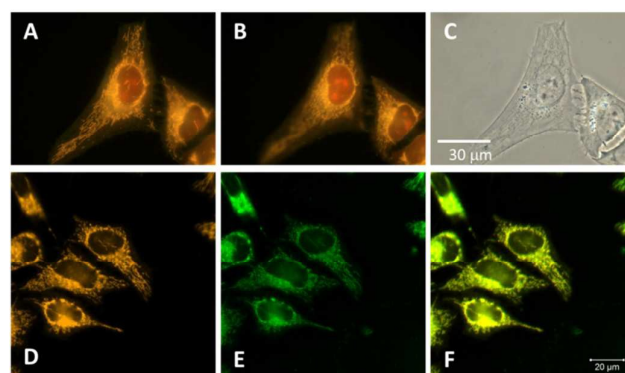


Fig. 4 (A and B) Fluorescent and (C) bright-field images of HeLa cells stained with ASCP (5 μM) for 30 min with focus at mitochondria (A) and nucleolus (B), respectively. $\lambda_{\text{ex}} = 460\text{--}490 \text{ nm}$; scale bar = 30 μm . (D and E) Confocal images of HeLa cells stained with (D) ASCP (5 μM) and (E) MitoTracker green (MTG; 200 nM). (F) The merged image of (D) and (E). Conditions: $\lambda_{\text{ex}} = 405 \text{ nm}$ and $\lambda_{\text{em}} = 600\text{--}700 \text{ nm}$ for ASCP; $\lambda_{\text{ex}} = 488 \text{ nm}$ and $\lambda_{\text{em}} = 500\text{--}540 \text{ nm}$ for MTG; scale bar = 20 μm .

The most abundant components in mitochondria and nucleolus are phospholipids and nucleic acids (DNAs and RNAs), respectively. To examine our hypothesis, phospholipids that found in the mitochondrial membrane (Chart S1, ESI[†]) and nucleic acids were chosen for mimicking the actual intracellular environment. Different lipid vesicles were first

fabricated as models of mitochondria by mixing desired ratio of phospholipids. The absorption and emission spectra of ASCP in the presence of lipid vesicles and nucleic acids in HEPES were then recorded. ASCP exhibits an absorption maximum at 435 nm in HEPES, showing no or little wavelength shift when treated with lipid vesicles. On the other hand, the absorption maximum of ASCP is red-shifted by 20 nm in the presence of nucleic acids (Fig. 5A). Similarly, while a 50 nm bathochromic shift in the emission maximum was observed when ASCP was mixed with nucleic acids, no change on the ASCP emission was observed by lipid vesicles (Fig. 5B). These results are consistent with the observations from fluorescent images as shown in Fig. 4A and 4B.

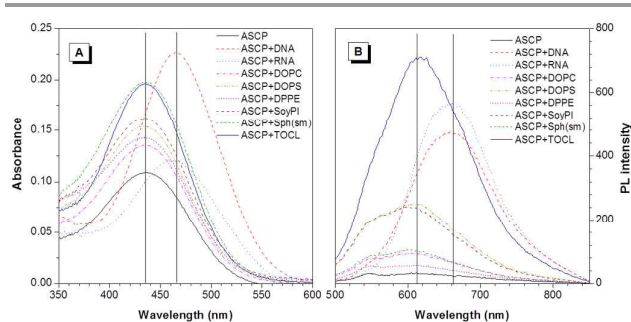


Fig. 5 (A) Absorption spectra and (B) emission spectra of ASCP mixed with different phospholipid vesicles, DNA and RNA in HEPES (pH 7.4) buffer solutions with 1% DMSO. Concentration: 10 μ M; λ_{ex} = 460 nm.

It becomes clear that why ASCP exhibits two different fluorescence in mitochondria and nucleolus. The next question is whether it is possible to use ASCP to collect individual fluorescence from mitochondria and nucleolus without cross contamination? To answer this, we attempted to collect the confocal images of dye-labelled HeLa cells by changing the excitation wavelengths and the emission filters. After optimizing the conditions, mitochondria can be visualized individually with orange fluorescence under 405 nm light excitation (Fig. 6A). On the other hand, only red fluorescence was observed in nucleoli at an excitation wavelength of 560 nm (Fig. 6B).

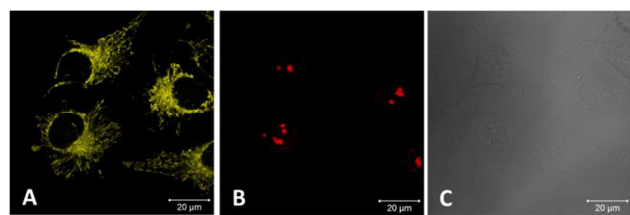


Fig. 6 (A and B) Confocal and (C) bright field images of HeLa cells stained with ASCP (5 μ M) for 30 min. Conditions: (A) λ_{ex} = 405 nm; λ_{em} = 500–650 nm; (B) λ_{ex} = 560 nm; λ_{em} = 650–750 nm.

3.4 Origin of Fluorescence in Nucleolus

Intercalation and electrostatic attraction are the possible interactions between ASCP and nuclei acids. When ASCP enters the cavities of nuclei acids, it may adopt a more co-

planar and conjugated conformation, and hence shows a redder emission. On the other hand, the hydrogen bonds between the nucleotides in nuclei acids may provide a relative polar environment for ASCP to emit at the longer wavelength region. In order to gain better understanding on the origin of red fluorescence, fluorescence imaging experiments were performed after the ASCP-labelled cells were fixed and treated with deoxyribonuclease (DNase) and ribonuclease (RNase). From the fluorescent images shown in Fig. 7, the specificity of ASCP to the nucleolus was lost when RNase was applied (Fig. 7B). However, the dye-labelled cells are still emissive after treated with DNase (Fig. 7C). The performance of ASCP was further verified by using SYTO RNaseSelect, a commercial fluorescent probe for nucleolus. As shown in Fig. 7E and 7F, SYTO RNaseSelect performed similar to ASCP. Since RNA contributes the major constituent in nucleolus, both ASCP and SYTO RNaseSelect tend to accumulate in nucleolus due to the strong electrostatic attraction. When the dye-labelled cells are treated with RNase, the binding sites for intercalation are collapsed and the dye molecules are now no longer bind to the RNA fragments. Thus, the fluorescent emission of ASCP and SYTO RNaseSelect in RNA-rich nucleolus is decreased dramatically.

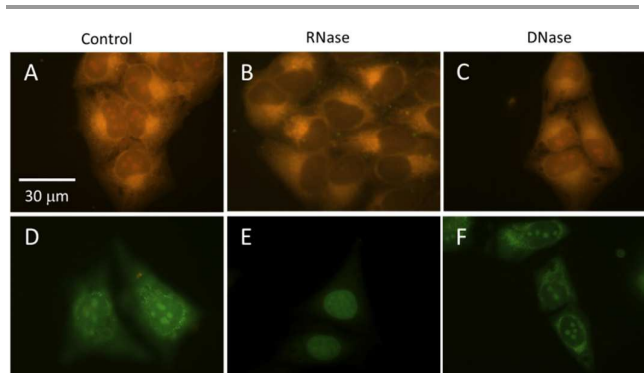


Fig. 7 Fluorescent images of HeLa cells stained with (A–C) ASCP (10 μ M) for 2 h and (D–F) SYTO RNaseSelect (5 μ M) for 2 h with or without treatment with RNase or DNase.

3.5 Photostability

Photostability is a critical important parameter for a fluorescent probe to find promising application in organelle imaging and tracking. To quantitatively investigate the photobleaching resistance of ASCP and SYTO RNaseSelect, continuous scanning of the dye-labelled cells by laser irradiation was carried out and the fluorescent signal at each scan was recorded. The dye-labelled cells were irradiated at 560 and 488 nm, respectively, with the same power. As shown in Figure 8, 5% fluorescence loss was observed in ASCP-stained cells after 50 scans. On the contrary, almost no fluorescent signal was detected from the cells stained with SYTO RNaseSelect after 15th scans. This result suggests that ASCP possesses a higher photo-bleaching resistance or photostability than SYTO RNaseSelect.

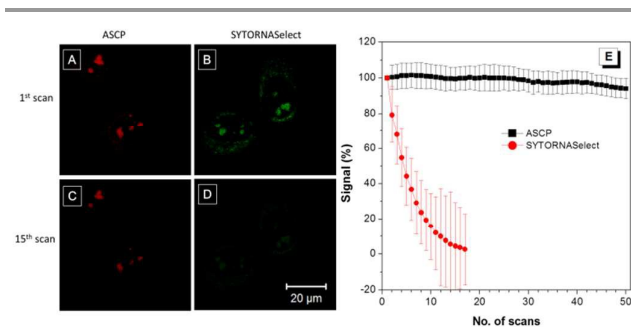


Fig. 8 Confocal images of HeLa cells stained with (A and C) ASCP and (B and D) SYTO RNASelect taken under continuous excitation. (E) Signal (%) of fluorescent emission of (black) ASCP and (red) SYTO RNASelect of different numbers of scan. Conditions: λ_{ex} = 560 nm and λ_{em} = 650–750 nm for ASCP; λ_{ex} = 488 nm, λ_{em} = 500–600 nm for SYTO RNASelect.

Conclusions

In summary, a dual-color organelle-specific probe with AIE feature for mitochondria and nucleolus is developed. Due to the different interactions with mitochondrial membrane and nuclei acids, distinct emission colors from mitochondria and nucleolus are observed under fluorescence microscopy. Owing to its high brightness, excellent biocompatibility and superior photostability, the AIE fluorescent probe is a promising candidate for simultaneous mitochondria and nucleolus imaging. Further studies on the development of AIEgens with multi organelle-specific emissions and exploration of their biomedical applications are ongoing in our laboratory.

Acknowledgements

This work was partially supported by the National Basic Research Program of China (973 Program, 2013CB834701 and 2013CB834702), the University Grants Committee of Hong Kong (AoE/P-03/08), the Research Grants Council of Hong Kong (16301614, 16305015 and N_HKUST604/14), the Innovation and Technology Commission (ITC-CNRC14SC01). We thank the support of the Guangdong Innovative Research Team Program (201101C0105067115).

Notes and references

- M. M. Yusupov, G. Z. Yusupova, A. Baucom, K. Lieberman, T. N. Earnest, J. H. D. Cate, H. F. Noller, *Science*, 2001, **292**, 883.
- Y. W. Lam, L. Trinkle-Mulcahy, A. I. Lamond, *J. Cell Sci.*, 2005, **118**, 1335.
- M. O. J. Olson, K. Hingorani, A. Szebeni, *Int. Rev. Cytol.*, 2002, **219**, 199.
- M. Carmo-Fonseca, L. Mendes-Soares, I. Campos, *Nat Cell Biol.*, 2000, **2**, E107.
- D. Hernandez-Verdun, P. Roussel, J. Gébrane-Younès, *J. Cell Sci.*, 2002, **115**, 2265.
- A. K. L. Leung, J. S. Andersen, M. Mann, A. I. Lamond, *Biochem. J.*, 2003, **376**, 553.
- U. Scheer, R. Hock, *Curr. Opin. Cell Biol.*, 1999, **11**, 385.
- R. Parlato, B. Liss, *Biochim. Biophys. Acta*, 2014, **1842**, 791.

- S. Boulon, B. J. Westman, S. Hutten, F. M. Boisvert, A. I. Lamond, *Mol. Cell*, 2010, **40**, 216.
- I. Johnson, M. T. Z. Spence, *Molecular probes handbook, A guide to fluorescent probes and labeling technologies*, 11th ed., *Invitrogen 2010*. Chapter 8, pp. 314.
- D. Honcharenko, C. Zhou, J. Chattopadhyaya, *J. Org. Chem.*, 2008, **73**, 2829.
- C. A. Alabi, K. T. Love, G. Sahay, T. Stutzman, W. T. Young, R. Langer, D. G. Anderson, *ACS Nano*, 2012, **6**, 6133.
- Y. Kam, A. Rubinstein, A. Nissan, D. Halle, E. Yavin, *Mol. Pharmaceutics*, 2012, **9**, 685.
- P. J. Santangelo, B. Nix, A. Tsourkas, G. Bao, *Nucleic Acids Res.*, 2004, **32**, e37.
- J. S. Paige, K. Y. Wu, S. R. Jaffrey, *Science*, 2011, **333**, 642.
- G. Bao, J. R. Won, A. Tsourkas, *Annu. Rev. Biomed. Eng.*, 2009, **11**, 25.
- I. E. Catrina, S. A. E. Marras, D. P. Bratu, *ACS Chem. Biol.*, 2012, **7**, 1586.
- P. Santangelo, N. Nitin, G. Bao, *Ann. Biomed. Eng.*, 2006, **34**, 39.
- Q. Li, Y. Kim, J. Namm, A. Kulkarni, G. R. Rosania, Y. H. Ahn, Y. T. Chang, *Chem. Biol.*, 2006, **13**, 615.
- G. Song, Y. Sun, Y. Liu, X. Wang, M. Chen, F. Miao, W. J. Zhang, X. Yu, J. Jin, *Biomater.*, 2014, **35**, 2103.
- J. T. Miao, C. Fan, R. Sun, Y. J. Xu, J. F. Ge, *J. Mater. Chem. B.*, 2014, **2**, 7065.
- M. Filosto, M. Scarpelli, M. S. Cotelli, V. Vielmi, A. Todeschini, V. Gregorelli, P. Tonin, G. Tomelleri, A. Padovani, *J. Neurol.*, 2011, **258**, 1763.
- A. Johri, M. F. Beal, *J. Pharmacol. Exp. Ther.*, 2012, **342**, 619.
- N. Zhao, M. Li, Y. Yan, J. W. Y. Lam, Y. L. Zhang, Y. S. Zhao, K. S. Wong, B. Z. Tang, *J. Mater. Chem. C*, 2013, **1**, 4640.
- M. Gao, Q. Hu, G. Feng, B. Z. Tang, B. Liu, *J. Mater. Chem. B*, 2014, **2**, 3438.
- Y. Li, Y. Wu, J. Chang, M. Chen, R. Liu, F. Li, *Chem. Commun.*, 2013, **49**, 11335.
- Q. Hu, M. Gao, G. Feng, X. Chen, B. Liu, *ACS Appl. Mater. Interfaces*, 2015, **7**, 4875.
- C. W. T. Leung, Y. Hong, J. Hanske, E. Zhao, S. Chen, E. V. Pletneva, B. Z. Tang, *Anal. Chem.*, 2014, **86**, 1263.
- D. R. Voelker, *Biochemistry of lipids, Lipoproteins and Membranes*, 4th Ed., 2002. Chapter 17.
- R. Hu, E. Lager, A. Aguilar-Aguilar, J. Liu, J. W. Y. Lam, H. H. Y. Sung, I. D. Williams, Y. Zhong, K. S. Wong, E. Pena-Cabrera, B. Z. Tang, *J. Phys. Chem. C*, 2009, **113**, 15845.

*For Table of Contents Use Only***A Photostable AIEgen for Nucleolus and Mitochondria Imaging with Organelle-Specific Emission**

A dual-color organelle-specific probe with AIE feature for mitochondria and nucleolus is developed. Due to the different interactions with mitochondrial membrane and nuclei acids, distinct emission colors from mitochondria and nucleolus are observed under fluorescence microscopy.

